Micro- and nanoelectronics. Condensed matter physics

Микро- и наноэлектроника. Физика конденсированного состояния

UDC 544.2
https://doi.org/10.32362/2500-316X-2021-9-5-57-66

RESEARCH ARTICLE

Evaporation of a liquid sessile droplet subjected to forced convection

Anna E. Korenchenko [1, @], Anna A. Zhukova [2]

[1] MIREA – Russian Technological University, Moscow, 119454 Russia
[2] Sechenov First Moscow State Medical University, Moscow, 105043 Russia
[@] Corresponding author, e-mail: korenchenko@mirea.ru

Abstract. The experiments on measuring the evaporation rate of liquid sessile droplets into air show that the rate of evaporation increases in the presence of forced convection flows. However, data on the effect of convection on the evaporation process is often contradictory and should be clarified. The paper presents a numerical analysis of evaporation from the surface of a water droplet subjected to forced convection in the gas phase. The drop is located on a smooth horizontal isothermal substrate; the mode with constant contact angle is considered. The form of the drop has axial symmetry, the same for the velocities and pressure. Forced convection compatible with the symmetry conditions are represented by flows directed downward along the axis of the system and diverging along the sides near the drop and the substrate. The mathematical model is constructed for evaporation controlled by diffusion in the gas phase and takes into account surface tension, gravity, and viscosity in both media, buoyancy and Marangoni convection. The results indicate the existence of the mutual influence of liquid and gaseous media. Thus, a drop vibrates under the influence of movements in the atmosphere, which generates a density wave in the gas: the drop "sounds". The magnitude of the velocity in a liquid is 50 times less than the characteristic velocity in air. It is found that the evaporation rate does not change in the presence of forced convection flows, which contradicts most of the experimental works. The reason for the discrepancies is supposed to be the appearance of nonequilibrium conditions at the boundary of the condensed phase, under which the evaporation regime ceases to be diffusional.

Keywords: evaporation, diffusion, sessile droplet, forced convection, mathematical modeling

• **Submitted:** 21.01.2021 • **Revised:** 01.03.2021 • **Accepted:** 12.07.2021

For citation: Korenchenko A.E., Zhukova A.A. Evaporation of a liquid sessile droplet subjected to forced convection. *Russ. Technol. J.* 2021;9(5):57–66. https://doi.org/10.32362/2500-316X-2021-9-5-57-66

Financial disclosure: The authors have no a financial or property interest in any material or method mentioned.

The authors declare no conflicts of interest.

НАУЧНАЯ СТАТЬЯ

Испарение жидкой лежащей капли в условиях вынужденной конвекции

А.Е. Коренченко [1, @], А.А. Жукова [2]

[1] *МИРЭА – Российский технологический университет, Москва, 119454 Россия*
[2] *Первый Московский государственный медицинский университет имени И.М. Сеченова, Москва, 105043 Россия*
[@] *Автор для переписки, e-mail: korenchenko@mirea.ru*

Резюме. Результаты экспериментов по измерению скорости испарения с поверхности жидкой лежащей капли в воздух указывают, что конвективные потоки над поверхностью увеличивают скорость испарения. Однако данные относительно того, в какой мере конвекция влияет на процесс испарения, сильно разнятся, часто противоречивы и требуют уточнения. В работе проведен численный анализ испарения с поверхности капли воды в нейтральный газ – воздух в присутствии конвективных течений в газовой фазе. Капля располагается на горизонтальной, гладкой, изотермической подложке, рассмотрена мода с постоянным углом смачивания. Задача решена в осесимметричном приближении, течения вынужденной конвекции, совместимые с условиями симметрии, представлены потоками, направленными вниз вдоль оси системы и расходящимися по сторонам вблизи капли и подложки. Математическая модель учитывает влияние сил поверхностного натяжения, тяготения и вязкости в обеих средах, возможную свободную гравитационную конвекцию в газовой и жидкой средах, конвекцию Марангони в капле и построена для испарения, контролируемого диффузией в газовой фазе. Получены результаты, свидетельствующие о взаимном влиянии жидкой и газовой сред: капля колеблется под влиянием движений в атмосфере, что порождает волну плотности в газе: колеблющаяся капля «звучит». Величина скорости в жидкой среде в 50 раз меньше характерной скорости в воздухе. Обнаружено, что скорость испарения не изменяется в присутствии течений вынужденной конвекции, что противоречит большинству экспериментальных работ. Предположительная причина расхождений заключается в возникновении неравновесных условий на границе конденсированной фазы, при которых режим испарения перестает быть диффузионным.

Ключевые слова: испарение, диффузия, лежащая капля, вынужденная конвекция, численное моделирование

• **Поступила:** 21.01.2021 • **Доработана:** 01.03.2021 • **Принята к опубликованию:** 12.07.2021

Для цитирования: Коренченко А.Е., Жукова А.А. Испарение жидкой лежащей капли в условиях вынужденной конвекции. *Russ. Technol. J.* 2021;9(5):57–66. https://doi.org/10.32362/2500-316X-2021-9-5-57-66

Прозрачность финансовой деятельности: Никто из авторов не имеет финансовой заинтересованности в представленных материалах или методах.

Авторы заявляют об отсутствии конфликта интересов.

INTRODUCTION

Evaporation of liquid from the surface of droplets is a part of the water cycle, is often encountered in everyday life, and is therefore actively studied theoretically and experimentally [1–6]. For surface evaporation of water, it was experimentally determined that convective air flows over the surface sometimes accelerate the evaporation, and that the evaporation is the more intense, the lower is the ambient humidity φ. However, the published data on the extent to which these phenomena affect the evaporation rate differ widely and are sometimes contradictory. For example, experimental studies of evaporation from the flat surface of water in the presence of convective flows showed an increase in the evaporation rate, which was characterized differently: as either linear in flow velocity V [7], or described by a polynomial of the third degree [8], or proportional to $\sim V^{3/2}$ [9], whereas numerical calculations indicated that the effect of convection on the evaporation rate is weak [2, 10]. The dependence of the evaporation rate

on the difference between the saturated vapor pressure over the surface (p_{vs}) and the partial vapor pressure in the surrounding air (p_{v0}) was experimentally described by a formula of the form $(p_{vs} - p_{v0})^n$, where the Dalton approximation predicted $n = 1$ [10], Tang and Etzion [7], and Al-Shammiri [9] obtained the n values smaller than 1, Boetler et al. [12] and Pauken et al. [13] calculated the n values larger than 1, and Jodat and Moghiman [8] proposed an expression relating n to the air flow velocity. Also different are opinions on the role of free convection in evaporation. Guéna et al. [14] experimentally investigated the evaporation rate from the surface of sessile and hanging water droplets and obtained equal values of the evaporation rate, which suggested the absence of the effect of gravitational convection in the gas phase. However, Kelly-Zion et al.'s in their experiments determined [15] that the evaporation rate from the surface of a sessile droplet is four times higher than that calculated for diffusion-controlled evaporation. Obviously, these contradictions are due to the fact that the conditions of the experiments [7–15] differed, but the reasons why the action of the same factors on evaporation brings about different responses are unclear.

Investigation of evaporation from the surface of a droplet requires one to take into account a lot of possible physical phenomena. For example, evaporation causes cooling of the droplet, which is generally nonuniform. This leads to a nonuniformity of the saturated vapor concentration over the surface, and also can lead to thermocapillary convection in the bulk of the droplet. Description of evaporation under gravity can be complicated by free convection in both the gas and the liquid media. Any external perturbations, mechanical or thermodynamic, can cause free vibrations of the droplet [16] and probably influence the evaporation. The main purpose of our studies is to numerically analyze the evaporation from the surface of a sessile droplet into a neutral gas. The calculations took into account the effect of the surface tension, gravity, and viscosity in both media, the possible free gravitational convection in the gas and liquid phases, and the Marangoni convection in the droplet. The effect of gravity on the shape of the droplet was also taken into account, and consideration was made of the movements of the surface of the droplet that are unrelated to the displacement of the droplet because of the decrease in the volume. We perform our analysis step by step; in this work, the effect of forced convection on the evaporation rate, the shape of the droplet, and the motion of its boundaries.

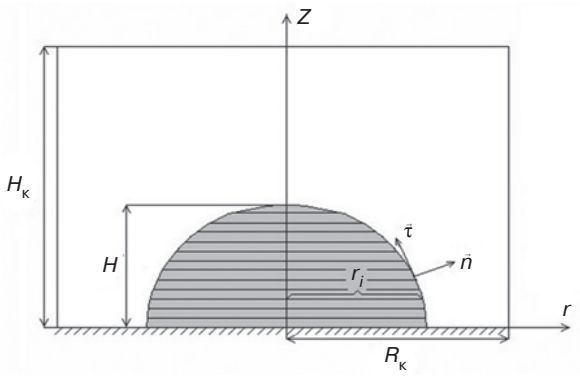

Fig. 1. Experimental design

1. DESCRIPTION OF MATHEMATICAL MODEL

1.1. Design of computer experiment and notation

Let us consider a liquid droplet lying on a horizontal surface, and let R be the radius of a spherical droplet of the same volume. The sessile droplet is in the atmosphere of a neutral noncondensable gas. The problem is solved in an axisymmetric assumption by the finite-difference method. The sizes of the computational space by far exceed the droplet radius: $R_{cs}, H_{cs} \gg R$ (Fig. 1 is sketchy, not to scale). A difference scheme is constructed as follows [16]: (1) the computational space at $z \le H$ is divided into horizontal layers so that the droplet is sliced into layers of equal thickness h_z with radius r_i; (2) the computational space in the gas above the droplet (at $z > H$) is also divided into horizontal layers of thickness, which may exceed h_z (not shown in Fig. 1); and (3) the computational space is divided into vertical layers (not shown in Fig. 1). Because of the complex shape of the subject of computation, the computational grid near the boundary of the droplet thickens to more accurately represent the shape of the boundary. The boundary of the droplet is given by a set of points (ih_z, r_i) connected by line segments.

The following notation is introduced: ρ_l is the density of the liquid; ρ_0, T_0, and p_0 are the density, temperature, and pressure of the gas at the boundaries of the computational space, respectively; T_s is the temperature of the substrate; ν_l and ν_g are the kinematic viscosities of the liquid and the gas, respectively; η_l and η_g are their dynamic viscosities; κ_l and κ_g are their thermal conductivities; c_l and c_g are their specific heat capacities; M_l and M_g are their molar masses; β_l is the thermal expansion coefficient of the liquid; D is the diffusion coefficient of the vapor in air; λ is the heat of evaporation; σ_{lg}, σ_{gs}, and σ_{ls} are the surface tensions at the liquid–gas, gas–solid, and liquid-solid interfaces, respectively. The subscripts l, g, and v refer to the liquid, the gas, and the vapor, respectively.

1.2. The main approximations of the model

It is assumed that the liquid is incompressible and Newtonian, the neutral gas and its mixture with the vapor are ideal gases, and the substrate is smooth and isothermal. The evaporation is assumed to be slow; therefore, over the surface of the liquid, there

is an equilibrium saturated vapor. A two-dimensional problem is considered under the assumption of the axial symmetry of the droplet, the flows, and the vapor pressure, temperature, and concentration distributions in the absence of flows of the media in the azimuthal direction.

1.3. Equations and boundary conditions

The conservation equations for the liquid in the droplet are written as follows:

$$\frac{\partial \vec{\mathbf{V}}}{\partial t}+\left(\vec{\mathbf{V}}\cdot\vec{\nabla}\right)\vec{\mathbf{V}}=-\frac{1}{\rho_l}\vec{\nabla}P+\nu_l\vec{\nabla}^2\vec{\mathbf{V}}-\vec{\mathbf{g}}\beta_l\left(T-T_s\right), \quad (1)$$

$$\vec{\nabla}\cdot\vec{\mathbf{V}}=0, \quad (2)$$

$$\frac{\partial T}{\partial t}+\vec{\nabla}\left(\vec{\mathbf{V}}T\right)=\frac{\kappa_l}{\rho_l c_l}\vec{\nabla}^2T. \quad (3)$$

Here, P is the excess of the pressure over the hydrostatic pressure in the liquid; $\vec{\mathbf{V}}=\{V_r, V_z\}$ and T are the velocity and temperature distributions, respectively; and $\vec{\mathbf{g}}$ is the acceleration of gravity. The buoyance in Eq. (1) is taken in to account in the Boussinesq approximation.

The behavior of the gas is described by the following equations:

$$\frac{\partial \vec{\mathbf{V}}}{\partial t}+\left(\vec{\mathbf{V}}\cdot\vec{\nabla}\right)\vec{\mathbf{V}}=-\frac{1}{\rho}\vec{\nabla}p+\frac{\eta_g}{\rho}\vec{\nabla}^2\vec{\mathbf{V}}-\vec{\mathbf{g}}, \quad (4)$$

$$\frac{\partial \rho}{\partial t}+\vec{\nabla}\left(\rho\vec{\mathbf{V}}\right)=0, \quad (5)$$

$$\frac{\partial T}{\partial t}+\vec{\nabla}\left(\vec{\mathbf{V}}T\right)=\frac{\kappa_g}{\rho c_g}\vec{\nabla}^2T, \quad (6)$$

$$\frac{\partial C}{\partial t}+\vec{\nabla}\left(\vec{\mathbf{V}}C\right)=D\vec{\nabla}^2C. \quad (7)$$

System (4)–(7) is supplemented with the equation of state of the vapor–gas mixture:

$$p=\frac{\rho R_g T}{M},\ M=\left(\frac{C}{M_l}+\frac{1-C}{M_g}\right)^{-1}. \quad (8)$$

Here, p, ρ, and M are the pressure, density, and molar mass of the mixture, respectively; C is the mass fraction of the vapor; and R_g is the universal gas constant.

The upper and lateral boundaries of the computational space are the unperturbed gas medium with given vapor mass fraction C_0, density ρ_0, pressure p_0, and temperature T_0.

At the gas–substrate interface, the impermeability, constant temperature, and no-slip conditions are specified.

At the liquid–gas interface S_{lg}, the following conditions are set [17]:

1) The partial vapor pressure p_{vs} is equal to the saturated vapor pressure of the liquid at the temperature of the surface and with taking into account the curvature $K(z)$ and the presence of the neutral gas:

$$p_{vs}=p_{v\infty}+\frac{\rho_{v\infty}}{\rho_l-\rho_{v\infty}}\left(-\sigma_{lg}K+p\right),$$

where $p_{v\infty}$ and $\rho_{v\infty}$ are the pressure and density of the vapor over the flat surface of the liquid ($K=\infty$), respectively; $p_{v\infty}$ is calculated as $p_{v\infty}=6.112e^{17.62(T_s-273)/(T_s-29.88)}$ [18]; and $p(z)$ is the air pressure over the surface of the droplet. The curvature is calculated from the expression $K\left(z_i\right)=R_{1i}^{-1}+R_{2i}^{-1}$; here, R_{1i} and R_{2i} are the radii of normal cross sections of the droplet, which are calculated from geometric considerations [16]. The mass fraction of the vapor over the surface of the droplet is found as

$$C_s=\frac{p_{vs}M_l}{\rho_s R_g T_s}, \quad (9)$$

where ρ_s is the density of the gas–vapor mixture over the surface of the droplet.

2) The normal component of the velocity of the gas medium over the surface of the droplet is determined by the Stefan condition:

$$(1-C_s)\cdot\left(\vec{\mathbf{V}}\cdot\vec{n}-V_{S_{lg}}\right)-D\frac{\partial(1-C)}{\partial n}=0. \quad (10)$$

Condition (10) is written in a frame of reference in which the interface is immovable and describes the diffusion-controlled evaporation: the diffusion air flow to the surface should be compensated for a convective flow from the surface; $V_{S_{lg}}$ is the velocity of the liquid–gas interface in a laboratory frame of reference.

3) The discontinuous change in the normal component of the tension at S_{lg} is described by the Laplace equation

$$\vec{n}\boldsymbol{T}\vec{n}\big|_l-\rho_l\left(\vec{V}_l\cdot\vec{n}-V_{S_{lg}}\right)^2-$$
$$-\left(\vec{n}\boldsymbol{T}\vec{n}\big|_g-\rho\left(\vec{V}_g\cdot\vec{n}-V_{S_{lg}}\right)^2\right)=\sigma_{lg}K, \quad (11)$$

where the components of the tension tensor $\boldsymbol{T}$ are written as $T_{ij} = -p\delta_{ij} + \eta\left(\partial u_i/\partial x_j + \partial u_j/\partial x_i\right)$, and δ_{ij} is the Kronecker delta.

4) The discontinuous change in the tangential component of the tension is equal to the tangential component of the surface tension gradient:

$$\vec{n}\boldsymbol{T}\vec{\tau}\big|_{\rm l} - \rho_{\rm l}\vec{V}_{\rm l}\cdot\vec{\tau}\left(\vec{V}_{\rm l}\cdot\vec{n} - V_{S_{\rm lg}}\right) -$$
$$-\left(\vec{n}\boldsymbol{T}\vec{\tau}\big|_{\rm g} - \rho\vec{V}_{\rm g}\cdot\vec{\tau}\left(\vec{V}_{\rm g}\cdot\vec{n} - V_{S_{\rm lg}}\right)\right) = -\left|\frac{d\sigma}{dT}\right|(\nabla T)_\tau. \quad (12)$$

Equation (12) assumes a linear dependence of the surface tension on temperature:

$$\sigma = \sigma_0 - \left|\frac{d\sigma}{dT}\right|\left(T - T_{\rm g}\right).$$

5) The tangential components of the velocity and the temperature at the interface is continuous:

$$V_{\rm l}\big|_\tau = V_{\rm g}\big|_\tau, \quad (13)$$

$$T_{\rm l} = T_{\rm g}. \quad (14)$$

6) The heat flux experiences a discontinuous change because of the absorption of the latent heat of evaporation:

$$-k_{\rm l}\frac{\partial T}{\partial n}\bigg|_{\rm l} + \rho_{\rm l}c_{\rm l}T_{\rm l}\cdot\left(\vec{\mathbf{V}}_{\rm l}\cdot\vec{n} - V_{S_{\rm lg}}\right) -$$
$$-\left(-k_{\rm g}\frac{\partial T}{\partial n}\bigg|_{\rm g} + \rho c_{\rm g}T_{\rm g}\cdot\left(\vec{\mathbf{V}}_{\rm g}\cdot\vec{n} - V_{S_{\rm lg}}\right)\right) = \dot{m}\cdot\lambda. \quad (15)$$

In Eq. (15), the local mass flux on the surface is expressed as

$$\dot{m} = \rho_{\rm l}\cdot\left(\vec{\mathbf{V}}_{\rm l}\cdot\vec{n} - V_{S_{\rm lg}}\right) =$$
$$= \rho C\cdot\left(\vec{\mathbf{V}}_{\rm g}\cdot\vec{n} - V_{S_{\rm lg}}\right) - \rho D\frac{\partial C}{\partial n} = \rho\cdot\left(\vec{\mathbf{V}}_{\rm g}\cdot\vec{n} - V_{S_{\rm lg}}\right). \quad (16)$$

The velocity of the interface is found from Eqs. (10) and (16) is written as

$$V_{S_{\rm lg}} = \left(\rho_{\rm l}\vec{V}_{\rm l}\cdot\vec{n} - \rho\vec{V}_{\rm g}\cdot\vec{n}\right)\Big/\left(\rho_{\rm l} - \rho\right)\Big|_{S_{\rm lg}}. \quad (17)$$

7) The condition at the three-phase boundary has the form

$$\theta_0 = \text{const}, \quad (18)$$

where θ_0 is the equilibrium contact angle: $\cos\theta_0 = \left(\sigma_{\rm gs} - \sigma_{\rm ls}\right)\big/\sigma_{\rm lg}$.

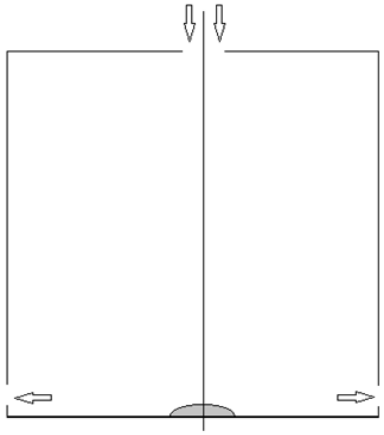

Fig. 2. Computational space (arrows show the air inlet and outlet zones)

To create forced convection flows compatible with the axial symmetry conditions, air is blown through an opening at the top of the computational space and leaves this space through a slot in the lateral walls at the bottom near the substrate (Fig. 2). The gas velocities were chosen so that the amounts of air and the vapor in the bulk remain unchanged during convection.

Equations (1)–(18) are nondimensionalized as follows. Of the parameters of the liquid, the distance is scaled relative to R; the velocity, $\nu_{\rm l}/R$; the pressure, $\rho_{\rm l}\nu_{\rm l}^2/R^2$; and time, $R^2/\nu_{\rm l}$. Of the parameters of the gas medium, the distance is scaled relative to $R_{\rm cs}$; the velocity, U_0; the density, ρ_g; and time, $R_{\rm cs}/U_0$. The dimensionless variables are hereinafter denoted by tildes.

2. NUMERICAL SOLUTION METHOD

System (1)–(18) was solved by the finite-difference method. Equations (1)–(3) of liquid dynamics were solved by the Gauss elimination method; the equations for the behavior of the gas medium were solved by the Thomas algorithm; and the solutions were joined at the interface using the boundary conditions. The solution procedure was inspired by split-step methods [19]: each time step was divided into a liquid characterization substep and a gas characterization substep, each of the substeps comprising several subsubsteps.

Substep 1: Liquid characterization. The equations for the liquid in the droplet are solved. Substep 1 consists of the following subsubsteps:

- the velocity and pressure distributions in the liquid are calculated by solving Eqs. (1), (2), (11), and (12) by the Gauss elimination method. The values of the velocities in the gas for substituting into Eqs. (11) and (12) are taken from the previous time step;

- the temperature distribution in the droplet is calculated by solving Eqs. (8) and (15). The temperature distribution in the gas and the evaporation intensity $\dot{m}$ are taken from the previous time step.

Substep 2: Gas characterization. Substep 2 consists of the following subsubsteps:

- the velocity distribution in the gas is calculated by solving Eqs. (4), (10), and (13); the normal components of the velocity in the gas near the surface of the liquid are given by the Stefan condition, and the tangential components thereof are continuous. The value of the gas density is taken from the previous time step, and the values of the tangential components of the velocities on the surface of the droplet are taken from substep 1 (liquid characterization);
- the density distribution in the gas is calculated by solving Eq. (5). Near the surface of the droplet, the density of the gas mixture is approximated by a polynomial because there are no physical conditions restricting the value of the density or its derivatives;
- the temperature distribution in the gas is calculated by solving Eqs. (6) and (14);
- the vapor mass fraction distribution in the gas is calculated by solving Eq. (7), in which the vapor mass fraction in the mixture over the surface of the droplet is calculated from formula (9);
- the new shape of the free liquid is calculated from formulas (18) and

$$\tilde{r}_i^{\tilde{t}+\Delta\tilde{t}} = r_i^{\tilde{t}} + \tilde{V}_r\big|_{S_{lg}} \cdot \Delta\tilde{t}, \quad i = 2,\ m,$$

$$\tilde{z}_i^{\tilde{t}+\Delta\tilde{t}} = i\tilde{h} + \tilde{V}_z\big|_{S_{lg}} \cdot \Delta\tilde{t}, \quad i = 2,\ m+1.$$

The computational grid is reconstructed at each time step according to the changes in the shape of the droplet. The variables for the liquid and the gas were nondimensionalized differently; therefore, there were several gas characterization substeps per liquid characterization substep.

The described code was tested on test problems [16, 20] and showed good agreement with analytical solutions and experimental results.

All the calculations in this work were performed for the evaporation of a droplet of water into air. The physical characteristics of the liquid are the following: the density is $\rho_l = 1000$ kg/m^3, the molar mass is $M_l = 0.018$ kg/mol, the thermal conductivity is $\kappa_l = 0.55$ W/(m·K), the viscosity is $\nu_l = 10^{-6}$ m^2/s, the specific heat capacity is $c_l = 4200$ J/(kg·K), the volumetric thermal expansion coefficient is $\beta_l = 1.27 \cdot 10^{-3}$ K^{-1}, and the heat of evaporation is $\lambda = 2.26 \cdot 10^6$ J/kg. The physical characteristics of the gas are the following: the molar mass is $M_g = 0.029$ kg/mol, the specific heat capacity is $c_g = 720$ J/(kg·K), the viscosity and thermal conductivity of the gas medium in Eqs. (4) and (6) were calculated from formulas of the kinetic theory of gases [21], and the diffusion coefficient of water vapor in air was calculated in an approximation of the hard-sphere model [22]. The temperature of the substrate was $T_s = 293$ K. The characteristics of the interfaces are the following: $\sigma_{lg} = 7.3 \cdot 10^{-2}$ N/m, $\sigma_{ls} - \sigma_{gs} = 0$ N/m, and $\left|\frac{d\sigma}{dT}\right| = 1.7 \cdot 10^{-4}$ N/(m·K). The sizes of the droplet and the computational space are $R = 0.5$ mm and $R_{cs} = H_{cs} = 5$ cm. The evaporation occurs in dry air: $C_0 = 0$.

The following values of the dimensionless numbers determining the motion in the liquid and the gas. The Marangoni number is $\mathrm{Ma} = 130$, which is sufficient to induce thermocapillary instability in the droplet because this value exceeds the critical value $\mathrm{Ma}_{cr} \approx 80$ (for a liquid film). The Reynolds numbers in the gas ($\mathrm{Re}_g = 115$) and in the liquid ($\mathrm{Re}_l = 0.5$) are relatively low; therefore, in both cases, only laminar flows can occur. The critical Grashof number is $\mathrm{Gr}_{cr} \approx 1000$ (for a liquid in a cylindrical vessel heated from below). This means that free gravitational convection in a droplet with $\mathrm{Gr} = 3.2$ is impossible.

The initial state of the system is the following: the media are at rest at temperature $T = T_s = T_0 = 293$ K; the pressure in the gas is $p = p_g = 10^4$ Pa; evaporation is absent, as if the droplet is covered with a film, and at time $t = 0$, the film is removed. The initial equilibrium shape of the droplet is calculated by minimizing the mechanical energy [16].

The convergence of the written code was checked by comparing the results obtained on various grids at various time steps, and the parameters of the scheme were chosen to obtain a solution that would be independent of computational step sizes.

3. RESULTS AND DISCUSSION

3.1. Flow patterns in the gas and the liquid

Forced convection flows were given as follows. At the upper boundary of the computational space at $z = H_{cs}$, there is round opening of radius $R_{air} = 5$ mm, through which dry air is blown (Fig. 2). The flow velocity profile is square: $V_z = U_0\left(1 - r^2/R_{air}^2\right)$, $U_0 = 0.37$ m/s. At the lateral boundary at $r = R_{cs}$, there

is a slot, through which air leaves the computational space; the width of the slot is chosen so the amount of air entering the space is equal to the amount of air leaving the space.

Three cases were calculated:

(1) the evaporation occurs into stagnant air;
(2) in the gas medium, there are forced convention flows, which exist from the initial time throughout the computational time range;
(3) in the gas medium, there are forced convection flows that are similar to those in case 2, with the difference that the former are pulsating; i.e., the state of forced convection as in case 2 is periodically replaced by the state in which the velocities at the inlet and outlet openings become zero. The movements in the gas, unsupported by external forces, rapidly die out.

Figure 3 shows the velocity distribution of the gas–vapor mixture over the droplet in case 2. The convective flow moves down along the axis of the system and diverges over the droplet. The velocities over the surface of the droplet are almost perpendicular to the surface. The component of these velocities that is normal to the surface is a Stefan flow. As Fig. 3 shows, the velocities of the convective flow over the droplet are twice and more as high as the velocity of the Stefan flow. Over the top of the droplet, a stagnant zone is formed where two vertical flows meet: the downward convective flow and the upward Stefan flow.

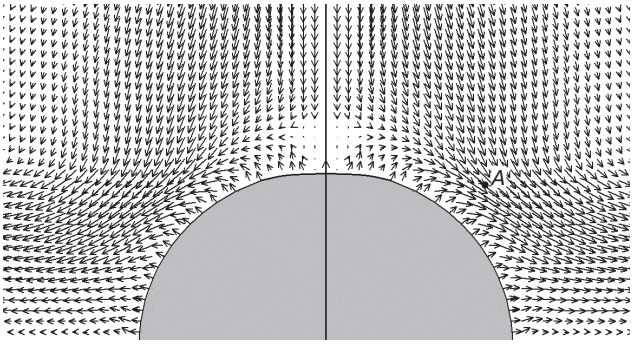

Fig. 3. Velocity distribution in the bulk of the gas near the surface of the droplet under forced convection conditions

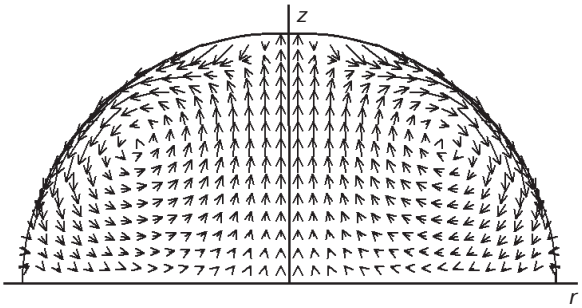

Fig. 4. Velocity distribution in the droplet under forced convection conditions in the gas phase

The convective flows in the gas cause motion inside the liquid. In the droplet, there is a vortex, the flow in which falls down along the surface of the droplet and rises up along the axis (Fig. 4). The velocities in the droplet are much lower than those in the gas. For example, the velocity of the flow in the gas at the point *A* (Fig. 3) is 5 cm/s, whereas the velocity of the flow in the droplet near the surface is about 1 mm/s, i.e., 50 times lower.

Figure 5 presents the time dependence of the deviation of the droplet height from the initial (equilibrium) value in two cases of evaporation: evaporation in the presence of pulsating forced convection flows and evaporation into stagnant air. Figure 5 also illustrates the time dependence of the forced convection velocity U_0; the period of pulsation of the convective flows was 0.5 s. It was determined that the droplet responses to the convection pulses by vibrations at a frequency of ~250 Hz, which is the eigenfrequency of the axisymmetric normal mode of the droplet [16]. Figure 5 shows that the mechanical equilibrium of the droplet is disturbed in both cases, in both the presence and the absence of convective flows. The droplet height in the presence of convective flows is smaller than that in the absence of convection; the difference is ~0.2 μm. This means that the convective flow flattens the droplet. As is seen from Fig. 5, in the stagnation intervals, when there are no convective flows, the droplet height is restored and becomes equal to the height of the droplet evaporating into stagnant air. The free vibrations under convection conditions have lower amplitude than in the absence of it; probably, they are suppressed by the convective flow.

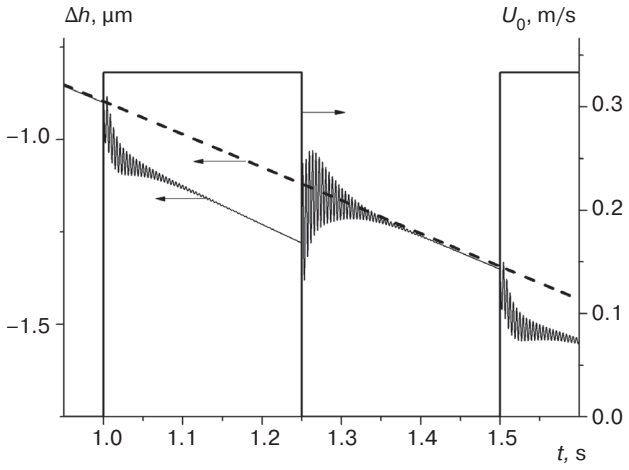

Fig. 5. Time dependence of the deviation of the droplet height at the top from the initial (equilibrium) value in cases 1 (dashed line) and 3 (semibold solid line), and the time dependence of the maximum air velocity in the convective flow (bold solid line)

There is also a feedback effect of the movement on the liquids on the gas. The vibrations of the

droplet give rise to a density wave in the gas; i.e., the vibrating droplet emits a sound. The density oscillations are low: their amplitude is about 0.01% of the air density.

3.2. Time dependence of the evaporation rate

Figure 6 shows the time dependence of the evaporation rate J, which is the mass of the liquid that leaves the surface of the droplet per unit time. Figure 6 presents three curves, each corresponding to one of the three considered evaporation cases. In the studied evaporation time range, one can see a short (<1 ms) transient process, during which the evaporation rate varies over a wide range. This is related to the nonequlibrium initial state of the system. Then, there is an interval of steady-state evaporation, in which the evaporation rate varies insignificantly—because of the decrease in the surface area of the droplet and in the surface temperature of it under the action of the evaporation. As is seen from Fig. 6, the curves at the stage of steady-state evaporation for different cases coincide with each other so that the difference does not exceed 1%. This confirms the conclusions made by authors of other computational works that the evaporation rate under the considered conditions is independent of the presence of convective flows in the gas phase [2, 10]; however, this contradicts the results of experimental studies of evaporation under forced convection conditions [8, 9, 15].

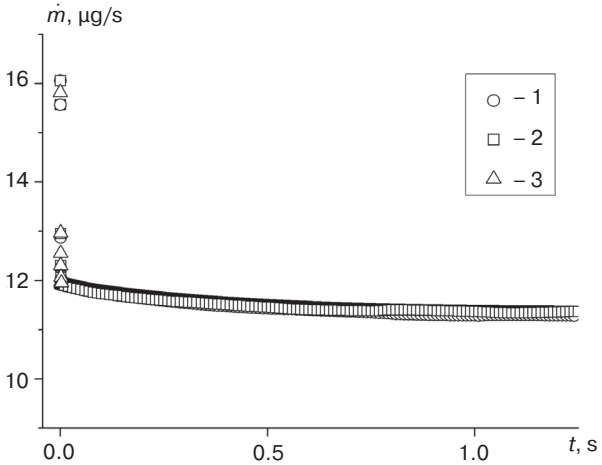

Fig. 6. Time dependence of the evaporation rate from the surface of the droplet in various evaporation cases

It was assumed that this disagreement is due to the fact that, in forced convection experiments, Stefan condition (10) is violated, whereas in numerical calculations, this condition is postulated. It is impossible to directly check whether or not the Stefan condition is valid in the experiment; however, there is indirect evidence that it is invalid. For example, the dependence of the evaporation rate from the surface of a droplet under diffusion control on the contact radius is a linear function [14, 15], and the fact that this condition is invalid suggests that the evaporation is not diffusion-controlled. Thus, the nonequilibrium conditions produced by the action of the convection on the surface of the droplet increase the evaporation rate.

CONCLUSIONS

The evaporation from the surface of a sessile droplet in the presence of forced convection flows in air was numerically studied, and the following results were obtained.

The forced convection in the gas phase affects the shape of the droplet and the flows in it. In the case of pulsating convective flows, the droplet responds to the beginning and end of the convection by vibrations at the eigenfrequency of its normal mode. After the vibrations die out, there is a flow in the droplet, which is caused by the flows in the surrounding air that are tangential to the surface of the droplet.

The curves of the time dependences of the evaporation rates in the cases of the evaporation into stagnant air and in the presence of forced convection flows coincide with each other, which agrees with the results of computational works [2, 10], but contradicts the data of experimental studies [7–9, 15]. It was assumed that this disagreement is due to the appearance of nonequilibrium conditions at the boundary of the condensed phase, under which the evaporation ceases to be diffusion-controlled. Thus, to numerically describe the effect of convection in the gas phase on the evaporation from the surface of a liquid, it is necessary to have a model of the interaction of flows with the matter in the Knudsen layer, at the boundary of which the obtained conditions should be joined with the systems of equations written for bulk regions.

Authors' contribution. All authors equally contributed to the research work.

REFERENCES

1. Borodulin V.Y., Letushko V.N., Nizovtsev M.I., Sterlyagov A.N. Determination of parameters of heat and mass transfer in evaporating drops. *International Journal of Heat and Mass Transfer*. 2017;109:609–618. https://doi.org/10.1016/j.ijheatmasstransfer.2017.02.042
2. Ljung A.-L., Lundström T.S. Evaporation of a sessile water droplet subjected to forced convection in humid environment. *Drying Technology*. 2019;37(1):129–138. https://doi.org/10.1080/07373937.2018.1441866
3. Kontorovich I.I. State of the art and development trends of technical decisions for intensifying evaporation from water surface. *Nauchnyy zhurnal Rossiyskogo NII problem melioratsii = Scientific Journal of Russian Scientific Research Institute of Land Improvement Problems*. 2016;1(21):241–256 (in Russ.).
4. Jeong S.W., Lee D.H. Drying performance of a dishwasher with internal air circulation. *Korean Journal of Chemical Engineering*. 2014;31(9):1518–1521. https://doi.org/10.1007/s11814-014-0194-0
5. Chen Y., Askounis A., Koutsos V., Valluri P., Takata Y., Wilson S.K., Sefiane K. On the effect of substrate viscoelasticity on the evaporation kinetics and deposition patterns of nanosuspension drops. *Langmuir*. 2020;36(1):204–213. https://doi.org/10.1021/acs.langmuir.9b02965
6. Hatte S., Pandey K., Pandey K., Chakraborty S., Basu S. Universal evaporation dynamics of ordered arrays of sessile droplets. *Journal of Fluid Mechanics*. 2019;866:61–81. https://doi.org/10.1017/jfm.2019.105
7. Tang R., Etzion Y. Comparative studies on the water evaporation rate from a wetted surface and that from a free water surface. *Building and Environment*. 2004;39(1):77–86. https://doi.org/10.1016/j.buildenv.2003.07.007
8. Jodat A., Moghiman M. An experimental assessment of the evaporation correlations for natural, forced and combined convection regimes. *Proceedings of the Institution of Mechanical Engineers Part C: Journal of Mechanical Engineering Science*. 2012;226(1):145–153. https://doi.org/10.1177/0954406211413961
9. Al-Shammiri M. Evaporation rate as a function of water salinity. *Desalination*. 2002;150(2):189–203. https://doi.org/10.1016/S0011-9164(02)00943-8
10. Vyatkin G.P., Korenchenko A.E., Izmailov Yu.G. Evaporation of liquids under conditions of free convection. *Doklady Physics*. 1998;43(11):700–702.
11. Dalton J. Experimental essays on the constitution mixed gases: on the force of steam or vapor from water and other liquids in different temperatures, both in a Torricelli vacuum and in air; on evaporation and on the expansion of gases by heat. *Memoirs of the Literary and Philosophical Society of Manchester*. 1802;5:536–602.
12. Boetler L.M.K., Gordon H.S., Griffin J.R. Free evaporation into air of water from a free horizontal quiet surface. *Industrial and Engineering Chemistry*. 1946;38(6):596–600. https://doi.org/10.1021/ie50438a018
13. Pauken M.T., Tang T.D., Jeter S.M., Abdel-Khalik S.I. Novel method for measuring water evaporation into still air. *ASHRAE Transactions*. 1993;99(1):297–300.

СПИСОК ЛИТЕРАТУРЫ

1. Borodulin V.Y., Letushko V.N., Nizovtsev M.I., Sterlyagov A.N. Determination of parameters of heat and mass transfer in evaporating drops. *International Journal of Heat and Mass Transfer*. 2017;109:609–618. https://doi.org/10.1016/j.ijheatmasstransfer.2017.02.042
2. Ljung A.-L., Lundström T.S. Evaporation of a sessile water droplet subjected to forced convection in humid environment. *Drying Technology*. 2019;37(1):129–138. https://doi.org/10.1080/07373937.2018.1441866
3. Конторович И.И. Уровень техники и тенденции развития технических решений для интенсификации испарения с водной поверхности. *Научный журнал Российского НИИ проблем мелиорации*. 2016;1(21):241–256.
4. Jeong S.W., Lee D.H. Drying performance of a dishwasher with internal air circulation. *Korean Journal of Chemical Engineering*. 2014;31(9):1518–1521. https://doi.org/10.1007/s11814-014-0194-0
5. Chen Y., Askounis A., Koutsos V., Valluri P., Takata Y., Wilson S.K., Sefiane K. On the effect of substrate viscoelasticity on the evaporation kinetics and deposition patterns of nanosuspension drops. *Langmuir*. 2020;36(1):204–213. https://doi.org/10.1021/acs.langmuir.9b02965
6. Hatte S., Pandey K., Pandey K., Chakraborty S., Basu S. Universal evaporation dynamics of ordered arrays of sessile droplets. *Journal of Fluid Mechanics*. 2019;866:61–81. https://doi.org/10.1017/jfm.2019.105
7. Tang R., Etzion Y. Comparative studies on the water evaporation rate from a wetted surface and that from a free water surface. *Building and Environment*. 2004;39(1):77–86. https://doi.org/10.1016/j.buildenv.2003.07.007
8. Jodat A., Moghiman M. An experimental assessment of the evaporation correlations for natural, forced and combined convection regimes. *Proceedings of the Institution of Mechanical Engineers Part C: Journal of Mechanical Engineering Science*. 2012;226(1):145–153. https://doi.org/10.1177/0954406211413961
9. Al-Shammiri M. Evaporation rate as a function of water salinity. *Desalination*. 2002;150(2):189–203. https://doi.org/10.1016/S0011-9164(02)00943-8
10. Vyatkin G.P., Korenchenko A.E., Izmailov Yu.G. Evaporation of liquids under conditions of free convection. *Doklady Physics*. 1998;43(11):700–702.
11. Dalton J. Experimental essays on the constitution mixed gases: on the force of steam or vapor from water and other liquids in different temperatures, both in a Torricelli vacuum and in air; on evaporation and on the expansion of gases by heat. *Memoirs of the Literary and Philosophical Society of Manchester*. 1802;5:536–602.
12. Boetler L.M.K., Gordon H.S., Griffin J.R. Free evaporation into air of water from a free horizontal quiet surface. *Industrial and Engineering Chemistry*. 1946;38(6):596–600. https://doi.org/10.1021/ie50438a018
13. Pauken M.T., Tang T.D., Jeter S.M., Abdel-Khalik S.I. Novel method for measuring water evaporation into still air. *ASHRAE Transactions*. 1993;99(1):297–300.
14. Guéna G., Poulard C., Voué M., De Coninck J., Cazabat A.M. Evaporation of sessile liquid droplets. *Colloids and Surfaces A: Physicochemical and Engineering Aspects*. 2006;291(1–3):191–196. https://doi.org/10.1016/j.colsurfa.2006.07.021

14. Guéna G., Poulard C., Voué M., De Coninck J., Cazabat A.M. Evaporation of sessile liquid droplets. *Colloids and Surfaces A: Physicochemical and Engineering Aspects*. 2006;291(1–3):191–196. https://doi.org/10.1016/j.colsurfa.2006.07.021
15. Kelly-Zion P.L., Pursell C.J., Vaidya S., Batra J. Evaporation of sessile drops under combined diffusion and natural convection. *Colloids and Surfaces A: Physicochemical and Engineering Aspects*. 2011;381(1–3):31–36. https://doi.org/10.1016/j.colsurfa.2011.03.020
16. Korenchenko A.E., Beskachko V.P. Oscillations of a sessile droplet in open air. *Physics of Fluids.* 2013;25(11):2106. https://doi.org/10.1063/1.4829025
17. Labuntsov D.A., Yagov V.V. *Mekhanika dvukhfaznykh sistem* (*The Mechanics of Two-Phase Systems).* Moscow: MEI; 2000. 374 p. (in Russ.). ISBN 978-5-383-00036-6
18. *Guide to Meteorological Instruments and Methods of Observation*. Geneva: World Meteorological Organization (WMO); 2008. 681 p. Available from URL: https://www.weather.gov/media/epz/mesonet/CWOP-WMO8.pdf
19. Belotserkovskii O.M. *Chislennoe modelirovanie v mekhanike sploshnykh sred* (*Numerical modeling in mechanics of continuous medium)*. Moscow: Fizmatlit; 1994. 448 p. (in Russ.). ISBN 5-02-014986-1
20. Korenchenko A.E., Malkova J.P. Numerical investigation of phase relationships in an oscillating sessile drop. *Physics of Fluids*. 2015;27(10):2104–2111. https://doi.org/10.1063/1.4932650
21. Matveev A.N. *Molekulyarnaya fizika* (*Molecular Physics)*. Moscow: Mir; 1985. 446 p. (in Russ.).
22. Bird R., Stewart W., Lightfoot E. *Transport Phenomena*. John Wiley & Sons, Inc.; 2002. 687 p.

15. Kelly-Zion P.L., Pursell C.J., Vaidya S., Batra J. Evaporation of sessile drops under combined diffusion and natural convection. *Colloids and Surfaces A: Physicochemical and Engineering Aspects*. 2011;381(1–3):31–36. https://doi.org/10.1016/j.colsurfa.2011.03.020
16. Korenchenko A.E., Beskachko V.P. Oscillations of a sessile droplet in open air. *Physics of Fluids.* 2013;25(11):2106. https://doi.org/10.1063/1.4829025
17. Лабунцов Д.А., Ягов В.В. *Механика двухфазных систем.* М.: МЭИ; 2000. 374 с. ISBN 978-5-383-00036-6
18. *Guide to Meteorological Instruments and Methods of Observation*. Geneva: World Meteorological Organization (WMO); 2008. 681 p. URL: https://www.weather.gov/media/epz/mesonet/CWOP-WMO8.pdf
19. Белоцерковский О.М. *Численное моделирование в механике сплошных сред*. М.: Физматлит; 1994. 448 с. ISBN 5-02-014986-1
20. Korenchenko A.E., Malkova J.P. Numerical investigation of phase relationships in an oscillating sessile drop. *Physics of Fluids*. 2015;27(10):2104–2111. https://doi.org/10.1063/1.4932650
21. Матвеев А.Н. *Молекулярная физика*. М.: Мир; 1985. 448 с.
22. Bird R., Stewart W., Lightfoot E. *Transport Phenomena*. John Wiley & Sons, Inc.; 2002. 687 p.

About the authors

Anna E. Korenchenko, Dr. Sci. (Phys.-Math.), Professor, Department of High Mathematics, Institute of Integrated Safety and Special Instrument Engineering, MIREA – Russian Technological University (78, Vernadskogo pr., Moscow, 119454 Russia). E-mail: korenchenko@mirea.ru. Scopus Author ID 10043443100, https://orcid.org/0000-0002-3413-8855

Anna A. Zhukova, Cand. Sci. (Chem.), Associate Professor, Sechenov First Moscow State Medical University (21, 5 Parkovaya ul., Moscow, 105043 Russia). E-mail: anyazhu@gmail.com. Scopus Author ID 12757009400, https://orcid.org/0000-0003-4511-1882

Об авторах

Коренченко Анна Евгеньевна, д.ф.-м.н., профессор, кафедра высшей математики Института комплексной безопасности и специального приборостроения ФГБОУ ВО «МИРЭА – Российский технологический университет» (119454, Россия, Москва, пр-т Вернадского, д. 78). E-mail: korenchenko@mirea.ru. Scopus Author ID 10043443100, https://orcid.org/0000-0002-3413-8855

Жукова Анна Александровна, к.х.н., доцент, кафедра аналитической, физической и коллоидной химии, Первый Московский государственный медицинский университет им. И.М. Сеченова (105043, Россия, Москва, 5-ая Парковая ул., 21). E-mail: anyazhu@gmail.com. Scopus Author ID 12757009400, https://orcid.org/0000-0003-4511-1882

Translated by V. Glyanchenko